4 Space Weather with Informatics, Information and Communications Technology

4-1 Technologies of Data Processing and Data Application

4-1-1 Development of Automatic Scaling Software of Ionospheric Parameters

KATO Hisao, TAKIGUCHI Yuka, FUKAYAMA Daigen, SHIMIZU Yukiko, MARUYAMA Takashi, and ISHII Mamoru

We have developed a new automatic scaling software of ionospheric parameters. Automatic monitoring of ionospheric irregularities has become more important since the ionospheric irregularities cause severe disturbances for recent sophisticated communication and navigation systems. NICT carries out a project to monitor the ionosphere in South-East Asia for early warning of occurrences of ionospheric irregularities. In this project, developing the automatic scaling software of ionogram occupies one of the important parts. In this paper, we report the new automatic scaling software of ionospheric parameters in detail. This software consists of noise reduction by wavelet transform and 2-D low-pass filter, detection of E/F-region echo traces, reduction of E/F-region multi-echoes and logical error omitting filter. We demonstrate its higher performance than old one by comparing automatically and manually scaled ionospheric parameters.

Keywords
Ionosphere, Ionospheric disturbances, Ionograms, Automatic scaling

1 Introduction

Satellite positioning has recently come into a growing range of advanced applications, including electronic navigation necessary for efficient aircraft operation and high-precision electronic surveying operable in mountainous areas with limited sight. In the meantime, disturbance phenomena occurring in the ionosphere at an altitude of 80 [km] to 1000 [km] are known to interfere with radio utilization. Therefore, gaining insight into ionospheric disturbance phenomena takes on increasing importance.

We have built a system for monitoring ionospheric disturbance phenomena in order to pursue a project for issuing early warning information. This project has deployed observational equipment, such as ionosondes, in Japan and Southeast Asia to monitor the ionospheric conditions. To expedite the issuance of warning information, ionospheric observational data (ionograms) must be analyzed and evaluated off-hand by automatically

scaling ionospheric parameter values.

The National Institute of Information and Communications Technology (as well as its predecessors) has been observing the ionosphere for more than 70 years. NICT placed an automatic ionospheric parameter scaling system [1][2] into service in the latter half of the 1980s. The system has since been upgraded to pursue higher stability with updated observation equipment and modified preprocessing sequences. NICT has now developed a scaling process that focuses on contour definition for the principal layers of the ionosphere (the E- and F-layers). This paper provides a summary report on the new scaling process with performance surpassing that of existing scaling programs [3].

2 System configuration and scaling process schematic

Figure 1 is a block diagram of the system.

Ionograms collected from ionospheric observation equipment installed at four nationwide observational facilities (at Wakkanai in Hokkaido, Kokubunji in Tokyo, Yamagawa in Kagoshima, and Ogimi in Okinawa) are processed into various forms and distributed to users on a near-real-time basis via existing servers. The automatic ionospheric parameter scaling software runs on the "new auto-scaling computer" shown in the diagram. This software has been developed with careful attention given to not interfering with existing program functionality.

Figure 2 schematically shows the sequence of scaling software processes.

As described later, input ionograms go

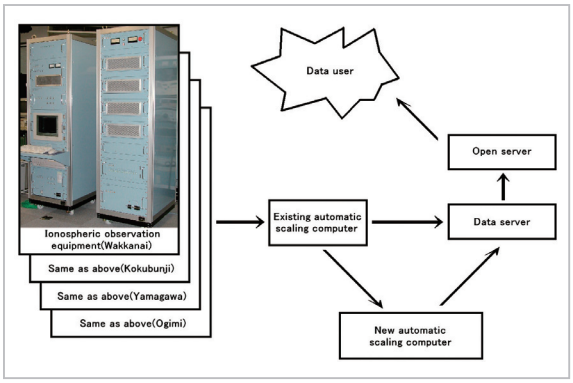

Fig.1 System block diagram

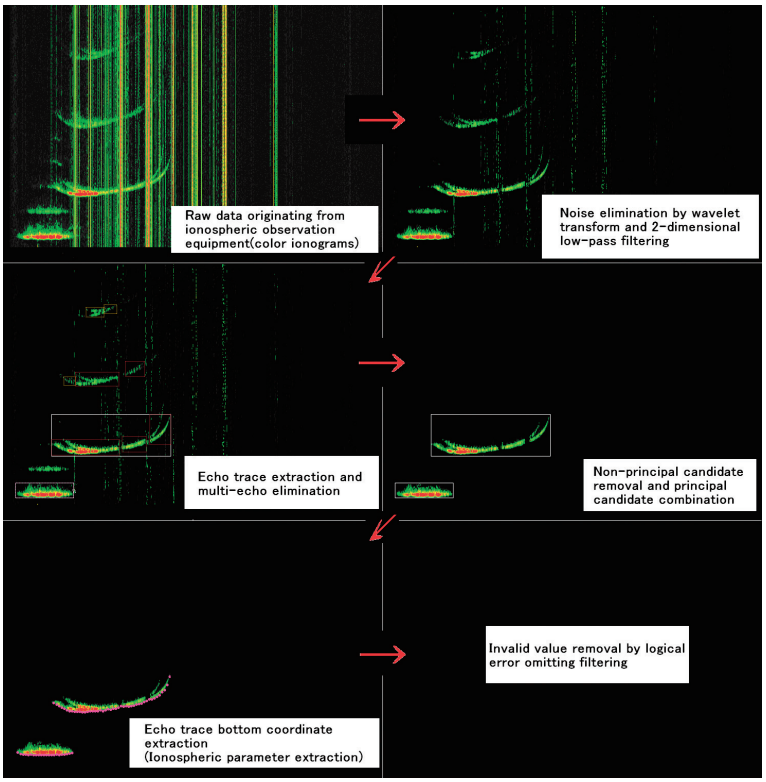

Fig.2 Process schematic

through a sequence of processes, such as a wavelet transform noise eliminator, two-dimensional low-pass filter noise eliminator, E/F-layer echo trace extractor, E/F-layer multi-echo eliminator, and a logical error omitting filter, before being subjected to automatic scaling.

3 Scaling software

Since observed ionograms contain a large amount of undesired components (such as noise and multi-echoes), most of the efforts toward developing this scaling software were directed at eliminating such undesired components.

Not all the processes yield equal processing results for all ionograms and side effects may be manifested; therefore, the work involved in developing and tuning software should dictate careful discretion.

3.1 Eliminating wavelet transform noise

While the large quantities of cross-modulation noise present in ionograms had traditionally been eliminated in a Fourier transform operation, this system employs a wavelet transform process to eliminate cross-modulation noise. Fourier transforms are vulnerable to a weakening of echo intensity due to harmonics being removed in the course of eliminating undesired components, as well as a hollowing of echoes due to an inability to detect echo components in case of saturated noise intensity. In contrast, the wavelet transform process takes about twice as long to process, but fits well with the tasks of extracting localized signals such as ionograms, thereby compensating for weaknesses of the Fourier transform process.

3.2 Eliminating 2D low-pass filter noise

Ionograms contain residual fine random noise even after the elimination of noise in a wavelet transform operation. Such noise can be effectively removed by using a two-dimensional low-pass filter for all pixels to identify the status of a particular pixel and adjacent pixels, and then remove the noise.

3.3 Extracting E-layer echoes

The following sequence of steps is conducted to extract E-layer echoes generally existing at an altitude of about 100 [km]:

(1) Define those regions having intensity not exceeding the threshold (default = 128, intensity, 8 bits = 0 to 255) and width in the frequency direction not exceeding the threshold (default = 3) as noise.
(2) Define those regions having width in the altitude direction greater than or equal to the threshold (default = 4) and width in the frequency direction less than the threshold (default = 10) as noise.
(3) From among the remaining regions, establish a central continuous area.
(4) Define those regions remote from the central continuous area in the frequency direction greater than or equal to the threshold (default = 40) as noise.
(5) Among the regions having width in the frequency direction less than the threshold (default = 10), define those regions not overlapping in the altitude direction from the central continuous area as noise.
(6) Assume that there is no E-layer when the total area of all regions is less than the threshold (default = 30).
(7) Define those regions having area less than the total region area threshold (default = 5%) as noise.
(8) Define those regions having area less than the threshold (default = 50) and less than the total region area threshold (default = 1%) as noise.

3.4 Eliminating E-layer multi-echoes

The following sequence of steps is conducted to eliminate E-layer multi-echoes arising from several runs of the reciprocal travel of observed waves between the E-layer and the ground:

(1) Determine an area of expected E-layer multi-echo appearance.
(2) Define those regions falling within the

expected appearance area as E-layer multi-echoes.
(3) Calculate a rate of protrusion for those regions in the vicinity of the expected appearance area protruding from that area.
(4) Define those regions having a rate of protrusion less than the threshold (default = 20%) as E-layer multi-echo.
(5) Set aside those regions having a rate of protrusion greater than or equal to the threshold (default = 80%), because they can be an F-layer.
(6) Define those regions having a rate of protrusion greater than or equal to the lower-limit threshold (default = 20%) and not exceeding the upper-limit threshold (default = 80%) as F-layer multi-echo, unless those regions overlap an F-layer echo.

3.5 Extracting F-layer echoes

The following sequence of steps is conducted to extract F-layer echoes generally existing at altitudes above 150 [km]:
(1) Define those regions having width in the altitude direction greater than or equal to the threshold (default = 10) and having width in the frequency direction less than the threshold (default = 10) as noise.
(2) Define those regions having width in the altitude direction greater than or equal to the threshold (default = 20) and having width in the frequency direction greater than or equal to than the threshold (default = 20) as an F-layer candidate.
(3) Define those regions having their width in the frequency direction greater than or equal to the threshold (default = 10) and having their intensity maximum greater than or equal to the threshold (default = 128) as a quasi-F-layer candidate.
(4) Define those fine vertical lines existing at other than both edges of each candidate and having width in the frequency direction not exceeding the threshold (default = 3) as noise.
(5) Combine two quasi-F-layer candidates meeting the relevant requirements and define that combination as an F-layer candidate if it meets the E-layer candidate requirements defined in (2) above.
(6) Combine an F-layer candidate and a quasi-F-layer candidate meeting the relevant requirements.
(7) Combine two F-layer candidates meeting the relevant requirements.
(8) In cases where only quasi-F-layer candidates exist, define those meeting the requirements of average intensity = maximum, area = maximum and regression analysis gradient = positive as F-layer candidates.
(9) Define those F-layer candidates falling within the threshold (default = 20) around the E-layer multi-echo region and having maximum intensity less than the threshold (default = 100) as part of E-layer multi-echo.

3.6 Eliminating F-layer multi-echoes

The following sequence of steps is conducted to eliminate F-layer multi-echoes arising from several runs of the reciprocal travel of observed waves between the F-layer and the ground:
(1) Determine an area of expected F-layer multi-echo appearance.
(2) Define those regions falling within the expected appearance area as F-layer multi-echo.
(3) In case of overlapping with an adjoining F-layer multi-echo, define only those regions falling within the expected appearance area as F-layer multi-echo.

3.7 Eliminating noise from the F-layer

The following sequence of steps is conducted to eliminate vertical-bar noise present in the F-layer candidate areas:
(1) Determine the inclination of the echo base, and define those areas having width in the frequency direction not exceeding the threshold (default = 15) and with initially negative inclination and positive ending inclination as vertical-line noise.
(2) If an area has initially negative inclination of the echo base at the leftmost edge of the echo, do not assume it as noise if there

is also initially negative inclination at the upper edge of the echo.

3.8 Selecting an F-layer from candidates

The following sequence of steps is conducted to select an optimal F-layer from among the F-layer candidates:

(1) Among all F-layer candidates, define the one having the largest area and maximum average intensity as an F-layer.
(2) In case none of the F-layer candidates meet the conditions in (1) above, determine the echo gradient for each F-layer candidate and eliminate those having a negative gradient.
(3) Among the remaining F-layer candidates, define the one existing at the lowest altitude and in the lowest frequency band as an F-layer.

3.9 Extracting ionospheric parameters

Sequencing the steps described above selects the regions of the E-layer and F-layer—the principal layers of the ionosphere. When the bottom trace coordinates of each region is extracted, followed by the maximum and minimum values in the altitude and frequency directions being determined, these values essentially form part of the ionospheric parameters cited in this paper as follows:

F-layer region minimum reflection frequency	fminF
F-layer region maximum reflection frequency	fmaxF
F-layer region minimum reflection altitude	hminF
E-layer region minimum reflection frequency	fminE
E-layer region maximum reflection frequency	fmaxE
E-layer region minimum reflection altitude	hminE

3.10 Logical error omitting filter

Because the processes introduced in the preceding sections make little allowance for the logical characteristics of the ionosphere, these processes may have extracted invalid values under the influence of residual noise in multi-echoes. Therefore, resultant trace information, altitude values and frequency values must be verified against the relevant ionospheric characteristics to eliminate logically impossible or doubtful values for enhanced accuracy.

4 Comparison results of automatically scaled values

Ionospheric parameter values (hereinafter "new auto-scaled values") thus obtained by automatic scaling have been verified against values calculated by running the existing automatic scaling programs (hereinafter "former auto-scaled values") and values calculated by human visual scaling (hereinafter "visual values") to determine the extent to which the new auto-scaled values are accurate.

To minimize verification errors associated with analyzer-specific visual value deviations, the range of errors in which matches are assumed has been set at ±25 [km] for altitude parameters and ±500 [kHz] for frequency parameters, in order to calculate a matching rate using the median of differences (defined as an offset) between visual values and auto-scaled values.

4.1 fmaxE

Ionospheric parameter "fmaxE," which denotes the maximum reflection frequency of E-layer echoes existing at an altitude of about 100 [km], has been compared and verified by using the maximum values of E-layer frequency for all new auto-scaled values, former auto-scaled values and visual values.

Figure 3 is a graph showing comparisons of fmaxE values observed at Kokubunji in March 2005.

In both the upper and lower panels, each red spot points to a visual value. Blue spots in the upper panel and lower panel indicate a former auto-scaled value and a new auto-scaled value, respectively. The new auto-scaled val-

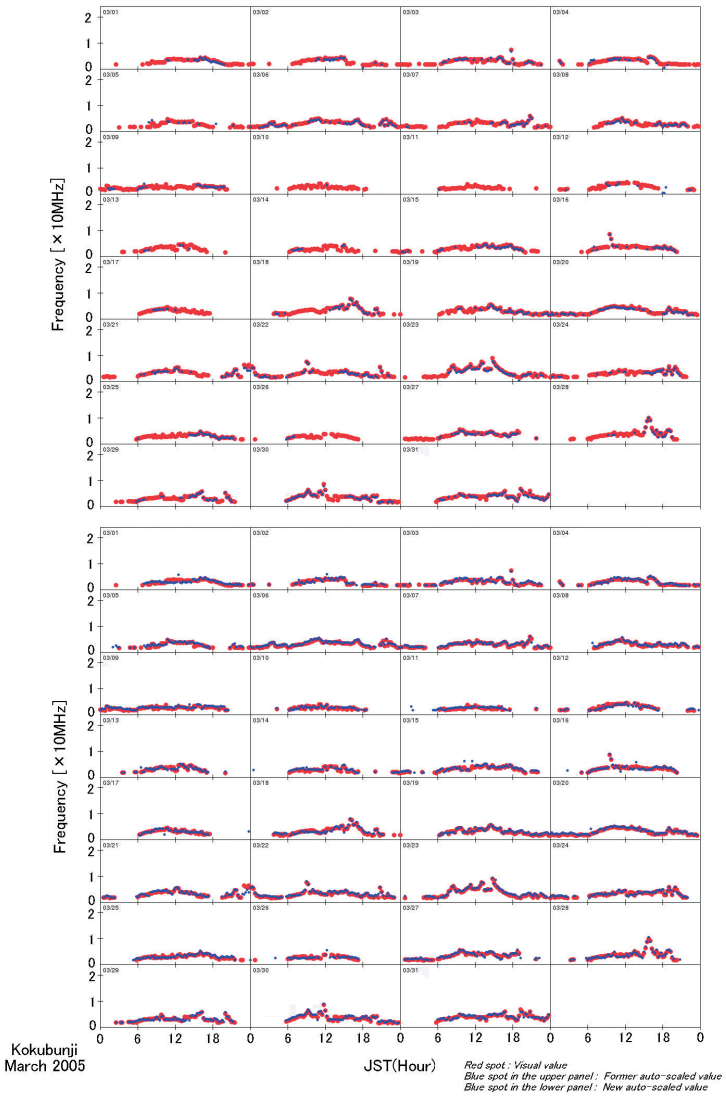

Fig.3 *fmaxE reading comparisons*

Red spot: a visual value, Blue spot in the upper panel: a former auto-scaled value, Blue spot in lower panel: a new auto-scaled value

Table 1 *Principal parameter reading and matching rate comparisons*

	fmaxE reading rate[%]			fmaxF reading rate[%]			hminF reading rate[%]		
	A	*B*	*C*	*A*	*B*	*C*	*A*	*B*	*C*
Jan. 2005	16	54	53	73	94	94	24	94	92
Feb. 2005	13	61	61	88	98	96	17	98	97
Mar. 2005	30	69	69	92	99	98	19	99	95
Apr. 2005	49	80	82	91	97	95	22	97	85
May. 2005	71	90	92	69	84	81	15	84	68
Jun. 2005	83	97	98	58	76	67	12	76	60
Jul. 2005	69	90	92	64	83	76	9	83	72
Aug. 2005	70	93	93	65	84	78	9	84	72
Sep. 2005	41	79	79	75	92	92	12	92	86
Oct. 2005	39	77	76	81	96	94	19	96	91
Nov. 2005	28	72	70	76	98	95	22	98	94
Dec. 2005	44	82	81	68	94	93	24	94	92

	fmaxE matching rate[%]		fmaxF matching rate[%]		hminF matching rate[%]	
	A	*B*	*A*	*B*	*A*	*B*
Jan. 2005	25	75	74	92	19	91
Feb. 2005	19	74	86	95	14	92
Mar. 2005	39	80	90	95	17	87
Apr. 2005	55	82	87	93	18	82
May. 2005	68	83	71	84	12	68
Jun. 2005	72	80	64	79	6	60
Jul. 2005	64	79	66	83	5	56
Aug. 2005	64	79	69	83	6	68
Sep. 2005	46	82	74	88	10	76
Oct. 2005	44	83	80	92	17	87
Nov. 2005	35	84	73	93	17	91
Dec. 2005	47	86	67	91	19	89

A : *Former auto-scaled value*
B : *New auto-scaled value*
C : *Visual value*

ues apparently demonstrate a high reading rate virtually equivalent to that of visual values. As indicated in Table 1, the matching rate has been drastically improved over that of the former auto-scaled values, averaging 80% or higher. Moreover, the visual values of fmaxE involve significant deviations associated with the analyzer's policy and other conditions, but a detailed retrospective review of the original ionograms has confirmed that the new auto-scaled values have higher accuracy than the matching rates listed in Table 1.

4.2 fmaxF

Ionospheric parameter "fmaxF," which denotes the maximum reflection frequency of F-layer echoes existing at an altitude of 150 [km] or higher, has been compared and verified by using the maximum values of F-layer frequency for all new auto-scaled values, former auto-scaled values and visual values.

The work of scaling F-layer parameter values involves particular difficulties in the summertime when sporadic E-layers dominate. This is because E-layer multi-echoes overlapping F-layer echoes could be mistakenly confused with F-layer echoes and retained, and part of the F-layer could also be confused with E-layer multi-echoes and removed.

Figure 4 presents a comparative graph for

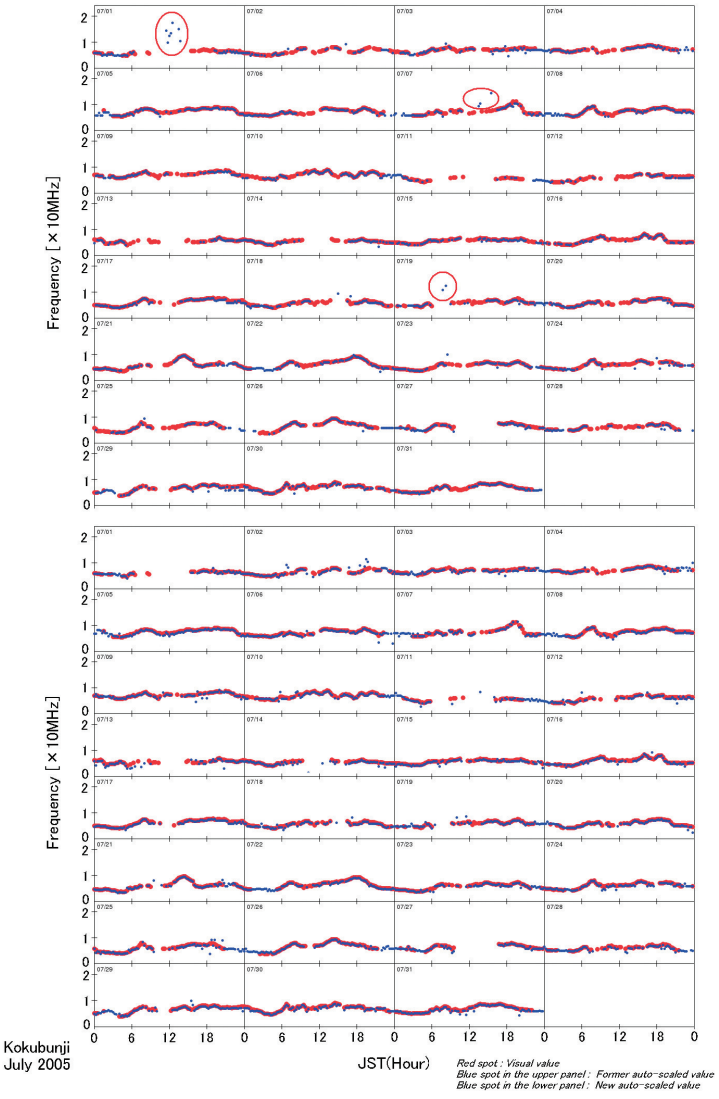

Fig.4 *fmaxF reading comparisons*

Red spot: a visual value, Blue spot in the upper panel: a former auto-scaled value, Blue spot in lower panel: a new auto-scaled value

Kokubunji in July 2005.

As shown in Table 1, the reading and matching rates of new auto-scaled values have generally improved 15% on average over those of the former auto-scaled values, with the average matching rate being close to 90%. The reading rate of new auto-scaled values sometimes exceeds the reading rate of visual values due to the possible "confusion over E-layer multi-echoes and F-layer echoes" as described above. As indicated by each red circle in Fig. 4, a prominent error involved in each former auto-scaled value has been effectively suppressed through the medium of the logical error omitting filter.

4.3 hminF

Ionospheric parameter "hminE," which denotes the maximum reflection altitude of the E-layer, has been compared and verified by using the minimum values of E-layer altitude for all new auto-scaled values, former auto-scaled values and visual values.

Figure 5 presents a comparative graph for Kokubunji in March 2005.

Both the reading and matching rates of new auto-scaled values have drastically improved over those of the auto-scaled values, but the work of scaling this parameter is difficult to achieve in the summer time for the same reason as explained for fmaxF. In addi-

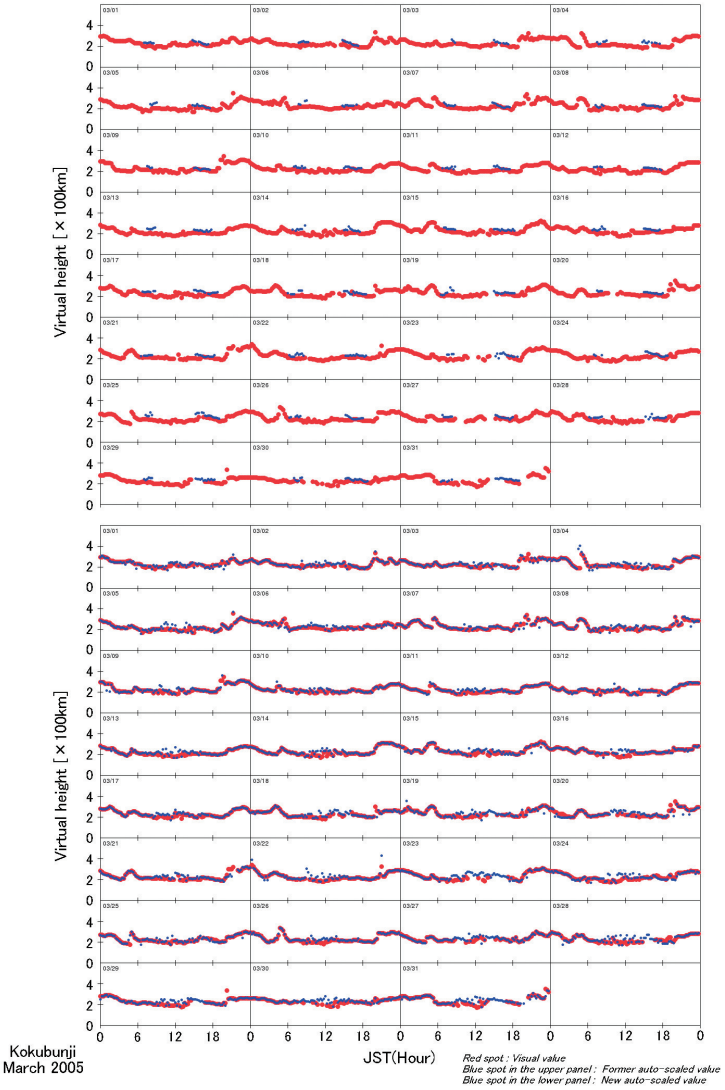

Fig.5 *hminF reading comparisons*

Red spot: a visual value, Blue spot in the upper panel: a former auto-scaled value, Blue spot in lower panel: a new auto-scaled value

tion, because the layer in which to scale hminF has a very high probability of overlapping E-layer multi-echoes, hminF is subject to degraded accuracy in the summertime when compared with other ionospheric parameters.

5 Real-time application of this software

Figure 6 shows a real-time application of the output yielded by running this automatic scaling software.

The diagram plots the estimated frequencies that can be propagated by communication point distance based on the transformation of echo trace information on each layer of an vertically observed ionospheric ionogram, in order to postulate "radio propagation by ionospheric reflection above a vertical observation point."

The plot covers "E-layer reflection over a communication point distance of 300 [km]." While the vertically observed ionospheric ionogram contains observational data with frequencies up to 30 [MHz], it suggests that E-layer reflections might make communication at frequencies up to 150 [MHz] possible, depending on the ionospheric conditions and the distance between communication points. From a different viewpoint, unpredictable interferences may have been induced over a distance between two communication points or in a frequency band that is normally beyond reach (e.g., FM broadcasting, TV analog terrestrial broadcasting, community disaster-preparedness radio communication).

6 Conclusions

As stated earlier, the advanced utilization of satellite positioning is now being pursued, thereby giving greater importance to the work of understanding ionospheric disturbance phenomena and disseminating resultant information. To this end, the automatic scaling of ionospheric parameter values is absolutely necessary. Because the new software developed this time focuses on extracting the principal layers of the ionosphere, making a distinction between the ordinary and extraordinary waves of echoes and between the F1 and F2-layers, and gaining detailed insight into ionospheric characteristics and phenomena such as echo dispersion are beyond the scope of this software. However, the use of this software has yielded performance far surpassing that of existing scaling programs as long as altitude and upper- and lower-limit frequencies are concerned. We are committed to continuing efforts not only to further upgrade our scaling program, but also for automatically detecting significant ionospheric phenomena, including but not limited to ionospheric storms that are to blame for satellite positioning errors and degraded satellite data communication, as well as sporadic E that induces extraordinary propagation of VHF signals and the Dellinger phenomenon that can disrupt marine and aeronautical radio communications and overseas broadcasting. In addition, resultant achievements will be posted at our Website and released through e-mail to disseminate warning information about ionos-

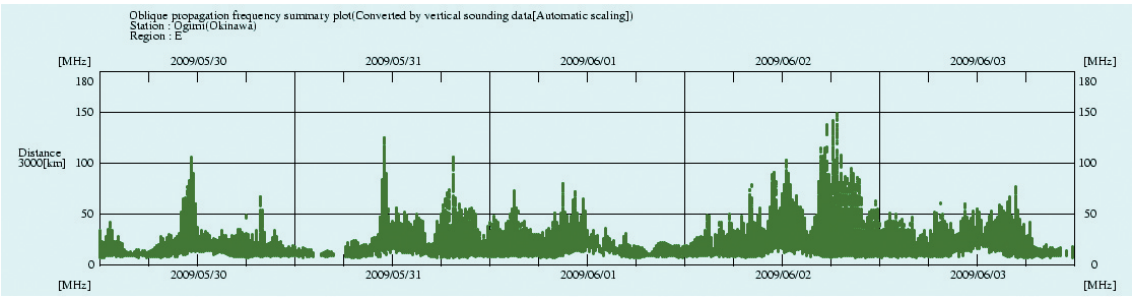

Fig.6 *Propagatable frequencies of long-haul communication estimated from auto-parsed parameter values*

pheric phenomena and their consequential social effects both extensively and promptly, thereby facilitating further advancements in space weather prediction.

References

1 Seiji Igi, Hisao Kato, and Makoto Yoshida, "Development of an automatic ionogram processing system, 5. Software at the central computer," Review of the Communications Research Laboratory, 35, 174, pp. 25–32, 1989. (in Japanese)

2 Seiji Igi, Tokuji Koizumi, Hisamitsu Minakoshi, and Makoto Yoshida, "Development of an automatic ionogram processing system, 7. Comparison between automatic and manual scaling of ionospheric parameters," Review of the Communications Research Laboratory, 35, 174, pp. 41–50, 1989. (in Japanese)

3 Makoto Yoshida, "Development of an automatic ionogram processing system, 6. Automatic scaling of ionospheric parameters," Review of the Communications Research Laboratory, 35, 174, pp. 33–40, 1989. (in Japanese)

KATO Hisao

Senior Researcher, Space Environment Group, Applied Electromagnetic Research Center

TAKIGUCHI Yuka

Information and Mathematical Science Laboratory, Inc.

***FUKAYAMA Daigen**, Ph.D.*

Research Center of Computational Mechanics,Inc.(Former address : Information and Mathematical Science Laboratory, Inc.)

Statistical Theory of Turbulence, Computational Thermodynamics

SHIMIZU Yukiko

YS CREATION (Former address : Information and Mathematical Science Laboratory, Inc.)

***MARUYAMA Takashi**, Ph.D. (Eng.)*

Executive Researcher

Upper Atmospheric Physics

***ISHII Mamoru**, Dr. Sci.*

Director, Project Promotion Office, Applied Electromagnetic Research Center

Upper Atmospheric Physics